

Article

Ductile Copolyesters Prepared Using Succinic Acid, 1,4-Butanediol, and Bis(2-hydroxyethyl) Terephthalate with Minimizing Generation of Tetrahydrofuran

Sang Uk Park, Hyeon Jeong Seo, Yeong Hyun Seo , Ju Yong Park, Hyunjin Kim, Woo Yeon Cho ,
Pyung Cheon Lee  and Bun Yeoul Lee * 

Department of Molecular Science and Technology, Ajou University, Suwon 16499, Republic of Korea; gkd13094@ajou.ac.kr (S.U.P.); hjseo@ajou.ac.kr (H.J.S.); tdg0730@ajou.ac.kr (Y.H.S.); pjy3741@ajou.ac.kr (J.Y.P.); khj610@ajou.ac.kr (H.K.); wycho418@ajou.ac.kr (W.Y.C.); pcleee@ajou.ac.kr (P.C.L.)

* Correspondence: bunyeoul@ajou.ac.kr; Tel.: +82-31-219-1844

Abstract: Poly(1,4-butylene succinate) (PBS) is a promising sustainable and biodegradable synthetic polyester. In this study, we synthesized PBS-based copolyesters by incorporating 5–20 mol% of $-O_2CC_6H_4CO_2-$ and $-OCH_2CH_2O-$ units through the polycondensation of succinic acid (SA) with 1,4-butanediol (BD) and bis(2-hydroxyethyl) terephthalate (BHET). Two different catalysts, H_3PO_4 and the conventional catalyst $(nBuO)_4Ti$, were used comparatively in the synthesis process. The copolyesters produced using the former were treated with $M(2\text{-ethylhexanoate})_2$ ($M = Mg, Zn, Mn$) to connect the chains through ionic interactions between M^{2+} ions and either $-CH_2OP(O)(OH)O^-$ or $(-CH_2O)_2P(O)O^-$ groups. By incorporating BHET units (i.e., $-O_2CC_6H_4CO_2-$ and $-OCH_2CH_2O-$), the resulting copolyesters exhibited improved ductile properties with enhanced elongation at break, albeit with reduced tensile strength. The copolyesters prepared with $H_3PO_4/M(2\text{-ethylhexanoate})_2$ displayed a less random distribution of $-O_2CC_6H_4CO_2-$ and $-OCH_2CH_2O-$ units, leading to a faster crystallization rate, higher T_m value, and higher yield strength compared to those prepared with $(nBuO)_4Ti$ using the same amount of BHET. Furthermore, they displayed substantial shear-thinning behavior in their rheological properties due to the presence of long-chain branches of $(-CH_2O)_3P=O$ units. Unfortunately, the copolyesters prepared with $H_3PO_4/M(2\text{-ethylhexanoate})_2$, and hence containing M^{2+} , $-CH_2OP(O)(OH)O^-$, $(-CH_2O)_2P(O)O^-$ groups, did not exhibit enhanced biodegradability under ambient soil conditions.

Keywords: PBS; poly(1,4-butylene succinate); bis(2-hydroxyethyl) terephthalate; copolyester; polycondensation; biodegradable



Citation: Park, S.U.; Seo, H.J.; Seo, Y.H.; Park, J.Y.; Kim, H.; Cho, W.Y.; Lee, P.C.; Lee, B.Y. Ductile Copolyesters Prepared Using Succinic Acid, 1,4-Butanediol, and Bis(2-hydroxyethyl) Terephthalate with Minimizing Generation of Tetrahydrofuran. *Polymers* **2024**, *16*, 519. <https://doi.org/10.3390/polym16040519>

Academic Editors: Joanna Rydz, Marta Musiol, Barbara Zawidlak-Węgrzyńska, Alena Opálková Šišková, Cristian Peptu and Darinka Christova

Received: 13 January 2024

Revised: 1 February 2024

Accepted: 8 February 2024

Published: 14 February 2024



Copyright: © 2024 by the authors. Licensee MDPI, Basel, Switzerland. This article is an open access article distributed under the terms and conditions of the Creative Commons Attribution (CC BY) license (<https://creativecommons.org/licenses/by/4.0/>).

1. Introduction

Polymers play an indispensable role in modern civilization, with annual production reaching approximately 400 million tons. However, their widespread use in various applications, including plastics, fibers, elastomers, coatings, and adhesives, is currently met with significant opposition due to concerns related to post-consumer waste and sustainability [1]. A staggering 30% of produced plastic waste is disposed of improperly, posing serious environmental challenges, and most of it is produced using fossil-based resources [2]. One promising approach to address these concerns is through closed-loop recycling of post-consumer polymers, often referred to as a circular economy [3–9]. However, in certain sectors, such as agriculture, recycling can be inherently challenging, making the promotion or enforcement of biodegradable polymers a viable alternative [10–12]. In this context, various types of biodegradable polymers have been explored [13–28]. While cellulose and starch-based polymers remain significant sources of biodegradable materials, there has been a recent surge in the production capacity of biodegradable synthetic polyesters like PBAT [poly(butylene adipate-co-terephthalate)] and PLA (polylactide) [29,30]. PLA, for

instance, is a sustainable polymer derived from renewable resources. However, it only composts under harsh artificial composting conditions and does not biodegrade at ambient conditions, limiting its acceptance in biodegradable polymer markets [2]. On the other hand, PBAT exhibits somewhat better biodegradability than PLA, with certain grades even receiving biodegradable certifications at ambient conditions [2]. However, it is important to note that raw materials used in PBAT production, particularly terephthalic acid and adipic acid, are currently derived from fossil-based sources.

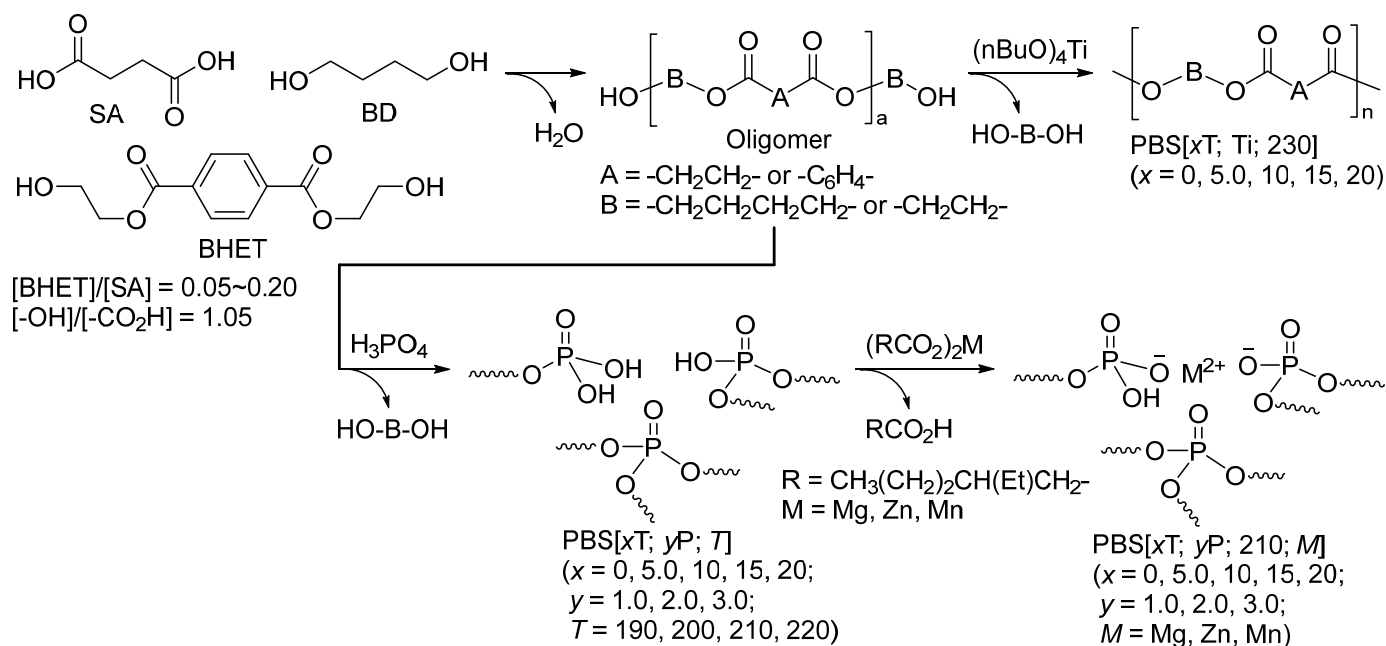
PBS stands as another promising sustainable and biodegradable synthetic polyester that has garnered significant attention from numerous companies aiming for commercialization [31–33]. However, its path to commercial success has not been as smooth as that of PLA and PBAT, and its accessibility remains somewhat limited. The primary obstacle to its widespread adoption may be attributed to the cost of the raw materials required for PBS production, namely, SA and BD. Currently, bio-based SA, a critical ingredient in PBS production, tends to be relatively more expensive compared to the fossil-based terephthalic acid and adipic acid utilized in the PBAT production. Nevertheless, there is mounting pressure to shift towards the production of bio-based polymers using monomers sourced from renewable resources [34]. This growing impetus has spurred considerable efforts towards the production of SA and BD through fermentation processes, leading to successful commercial production initiatives that have been announced and are currently expanding [35–37].

PBS is a semi-crystalline polymer known for its melting temperature (T_m) of approximately 115 °C. It has traditionally been characterized as a brittle polymer with a high tensile strength ranging from 20 to 30 MPa but a low elongation at break, typically below 100% [38–40], even though there are reports indicating significantly higher tensile strengths of 59 and 42 MPa accompanied by excellent elongation at break values of 700 and 230% [41,42]. In pursuit of either altering its mechanical properties or reducing production costs, researchers have synthesized various derivatives of PBS such as poly(butylene succinate-*co*-adipate) (PBSA) [43,44], poly(butylene succinate-*co*-terephthalate) (PBST) [40,45,46], poly(butylene succinate-*co*-furandicarboxylate) [47], poly(butylene succinate-*co*-2-methylsuccinate) [39], poly(butylene succinate-*co*-isosorbide succinate) [24], poly(butylene succinate-*co*-ethylene succinate) [41,48], poly(butylene succinate-*co*-caprolactone) [49], PBS-*block*-poly(butylene terephthalate) [50], PBS-*block*-polydimethylsiloxane [51], and PBS containing side chain onium salts [52], providing insights into their distinctive properties.

Typically, PBS and its derivatives have been synthesized by $(RO)_4Ti$ -catalyzed diacid/diol polycondensation. However, the molecular weights attainable by the polycondensation are reported to be limited, $M_w < 100$ kDa, due to simultaneous occurrence of competing reactions of polycondensation and degradation at the latter stage [53,54], and chain extension reactions have been performed at the final stage of polycondensation [55,56]. Many articles suggested the use of a diisocyanate such as 1,6-hexamethylene diisocyanate (HDI) as a chain-extending agent. However, the disadvantage is that the chain extender integration tends to reduce biodegradability [53,57]. Recently, we have pioneered a novel approach for the synthesis of rapidly biodegradable polyesters [58]. In this method, chain extension is achieved through ionic bonds formed between phosphate groups [$\sim OP(O)(OH)O^-$ or $(\sim O)_2P(O)O^-$] and divalent metal ions, such as Zn^{2+} or Mg^{2+} . The process involves the facile synthesis of polyesters containing phosphate groups [$\sim OPO(OH)_2$ or $(\sim O)_2P(O)OH$] by simply substituting the $(RO)_4Ti$ catalyst with H_3PO_4 during the polycondensation. These resulting PBATs exhibit significantly enhanced biodegradability, making them potentially useful as slow-releasing fertilizers during composting due to their content of plant growth nutrients—phosphate and metal ions [59,60].

In this study, we have extended our innovative approach by synthesizing PBS derivatives. Specifically, we carried out the SA/BD polycondensation process in the presence of an additional compound, BHET, with the aim of imparting ductile properties and evaluating biodegradability (Scheme 1). In a prior communication [58], it was demonstrated that the ionic aggregates of PBS, where chains are elongated with phosphate groups and divalent

metal ions, displayed brittle characteristics with an elongation at break of only 20%, and its biodegradability was not assessed. BHET is recognized as a crucial intermediate in the closed-loop recycling of poly(ethylene terephthalate) (PET). Waste PET is converted into BHET, which can then be transformed back into PET, making it a potentially abundant and cost-effective chemical resource for the near future [61–63]. Incorporating terephthalate units into aliphatic polyesters or aliphatic polycarbonates is typically crucial in enhancing their thermal and mechanical properties [64]. However, the direct utilization of terephthalic acid or dimethyl terephthalate in the polycondensation process presents challenges due to their intractability or sublimation tendencies. The use of BHET offers a solution to circumvent these issues.



Scheme 1. H_3PO_4 -catalyzed and conventional $(\text{nBuO})_4\text{Ti}$ -catalyzed SA/[BD + BHET] polycondensation.

2. Materials and Methods

2.1. General Remarks

Phosphoric acid (85.0%), SA ($\geq 99.0\%$), $(\text{nBuO})_4\text{Ti}$ (97%), and $\text{Mg}(\text{OH})_2$ were purchased from Sigma-Aldrich (St. Louis, MO, USA). BD (99.5%, 18 L scale) was purchased from Duksan (Reagents Duksan, Ansan, Korea). 2-Ethylhexanoic acid was purchased from TCI (Tokyo, Japan). $\text{Zn}(\text{2-ethylhexanoate})_2$ (80 wt% in mineral spirits), and $\text{Mn}(\text{2-ethylhexanoate})_2$ (40 wt% in mineral spirits) were purchased from Alfa Aesar (Ward Hill, MA, USA). ^1H NMR (600 MHz), ^{13}C NMR (150 MHz), and ^{31}P NMR (243 MHz) analyses were performed by using a JEOL ECZ 600 instrument (JEOL, Tokyo, Japan). The GPC data were obtained in CHCl_3 at 40°C using a Waters Millennium apparatus with polystyrene standards. The T_m , T_g , T_c , T_{cc} and their enthalpy (ΔH) data were determined with DSC 200 F3 Maia (NETZSCH, Bavaria, Germany) at a heating rate of $10^\circ\text{C}/\text{min}$. For tensile studies, the polymer samples were compressed between hot plates at 130°C . The pressure was applied incrementally, starting from 1 MPa to 5 MPa, with each 1 MPa increment lasting 5 min, totaling 20 min. Subsequently, the pressure was increased from 5 MPa to 10 MPa, with each 1 MPa increment lasting 10 min, accumulating to a total duration of 60 min. Tensile tests were performed according to ASTM D882 [65] using a Instron 3367 UTM (Instron, MA, USA) at a drawing rate of 50 mm/min with a gauge length of 50 mm.

2.2. Preparation of Mg(2-Ethylhexanoate)₂

Mg(OH)₂ (39.5 g, 0.644 mol) and 2-ethylhexanoic acid (371 g, 2.57 mol, 4.0 equivalents) were placed in a 500 mL reaction vessel equipped with a mechanical stirrer. The reactor was connected to a manifold and evacuated for 30 min. After filling it with N₂ gas, the heating mantle's temperature was set to 80 °C. All solids dissolved within 4 h. The temperature was then reduced to 60 °C, and the generated water was removed by evacuation (0.3 mmHg) for 12 h. This process yielded a viscous oil (193 g, constituting 50 wt% in 2-ethylhexanoic acid), which was used as obtained.

2.3. Preparation of PBS[5.0T; 1.0P; 210; Mg]

BD (90.1 g, 1.00 mol), SA (118 g, 1.00 mol), and BHET (12.7 g, 50 mmol, 5.0 mol% per succinic acid) were placed into a 500 mL reaction vessel equipped with a mechanical stirrer and a distillation setup. After a 30 min evacuation, the reactor was purged with N₂ gas. The esterification reaction was initiated by heating to 190 °C using the heating mantle and was allowed to proceed for 3 h, during which water was continuously removed through the distillation setup equipped with a receiver. To collect any distillates, the receiver was cooled using a dry ice/acetone bath, while the pressure was equalized to atmospheric pressure through a mercury bubbler. H₃PO₄ (85 wt%, 1.15 g, 10 mmol) was then added using a syringe. Subsequently, the receiver flask (250 mL) used for collecting water during the esterification reaction was replaced with an empty one (100 mL) under a nitrogen flux. While maintaining the temperature at 190 °C, the evacuation level was gradually increased over 1 h until full evacuation was achieved (0.3–0.4 mbar). Next, the heating mantle temperature was raised to 210 °C, and polycondensation was carried out under full evacuation for 4 h. As the molecular weight increased, the stirring rate of our mechanical stirrer was automatically decreased from 250 to 60 rpm. The reactor was purged with N₂ gas, and Mg(2-ethylhexanoate)₂ was introduced into the reactor using a syringe. Volatile components (2-ethylhexanoic acid) generated during this step were removed through full re-evacuation at a mantle temperature of 210 °C for 1 h, eventually reaching a stirring rate of 1–3 rpm. The polymer melt was extracted from the reactor while it was still hot, and it was subsequently cut into pieces using a paper cutter before being allowed to fully crystallize.

2.4. Preparation of PBS[5.0T; Ti; 230]

The esterification process was conducted using the same equipment and chemicals as those used in the preparation of PBS[5.0T; 1.0P; 210; Mg]. After introducing (nBuO)₄Ti (0.24 g, 0.72 mmol) with a syringe, the evacuation level was gradually increased at 190 °C over the course of 1 h until full evacuation was achieved (0.3–0.4 mbar). Subsequently, polycondensation was carried out at a mantle temperature of 230 °C for 4 h, finally reaching a state where the operation of the mechanical stirrer was halted. Finally, H₃PO₄ (85 wt%, 0.080 g, 0.82 mmol, 1.15 equivalents per (nBuO)₄Ti) was introduced using a syringe to deactivate the Ti catalyst, following a purge with N₂ gas. The resulting polymer melt was handled in the same manner as the preparation of PBS[5.0T; 1.0P; 210; Mg].

2.5. Biodegradation Studies

Soil samples were collected from three locations in South Korea for biodegradability assays: Mt. Gwanggyosan, Suwon (37°20.1360 N 127°1.1640' E); Ajou University's field campus, Suwon (37°17.1210 N 127°2.6710 E); and Hwaseong flower beds (37°10.8030 N 126°58.8720 E), following ISO 17556 [66] guidelines. The soil was air-dried, homogenized, and sieved (2 mm mesh). PBS[5.0T; 1.0P; 210; M] (M = Mg, Zn, Mn) were ground and sieved (2 mm mesh) using a Type ZM 200 Ultra Centrifugal Mill (Retsch, Haan, Germany). Each reactor contains a mixture of 5 g PBS derivative, 800 g soil, 200 mL distilled water, and nutrients (0.2 g KH₂PO₄, 0.1 g MgSO₄, 0.4 g NaNO₃, 0.4 g CO(NH₂)₂, 0.4 g NH₄Cl per kg soil), incubated aerobically at 25 °C in the dark using a 12-channel ECHO[®] respirometer (ECHO Instruments, Slovenske Konjice, Slovenia). Microcrystalline cellulose (20 μm, Sigma-

Aldrich, USA) was used as a control, prepared under similar conditions. Blank soil samples were also prepared to normalize the evolved CO₂. CO₂ evolution within the reactors was continuously monitored in real-time using a near-infrared (NIR) detector in the ECHO[®] system. The system maintained an airflow rate of 200 mL/min, which was regulated by an integrated mass flow controller.

3. Results and Discussion

3.1. SA/(BD + BHET) Polycondensation

Conventionally, the synthesis of PBS involves a two-step process. The first step is the esterification of SA and BD, which takes place at atmospheric pressure with continuous removal of generated H₂O without the need for an additional catalyst. This step results in the formation of an oligomer containing –OH end groups. The second step involves a transesterification reaction with the removal of the generated BD under evacuation conditions. Typically, titanium alkoxide [(RO)₄Ti] is used as the catalyst in this step [53]. To ensure the formation of oligomers containing –OH end groups, an excess of BD is added relative to SA. In our experiments, we performed the SA/BD esterification reaction by introducing additional BHET at 190 °C for 3 h with removal of any generated water. The quantity of BHET added was varied at 5, 10, 15, and 20 mol% per SA, while adjusting the amount of BD to maintain an [–OH]/[–CO₂H] ratio of 1.05. Subsequently, we carried out the polycondensation with feeding H₃PO₄ (1.0, 2.0, or 3.0 mol% per SA), replacing the conventional (RO)₄Ti catalyst, and with gradually increasing the evacuation level over 1.0 h, ultimately reaching a full vacuum state. The polycondensation process was then continued under full evacuation, with the removal of the generated BD or, if present, ethylene glycol, at elevated temperatures of 200, 210, or 220 °C to obtain thick and viscous polymer melts.

The ³¹P NMR spectra clearly indicate that H₃PO₄ not only acted as a catalyst during the polycondensation process but was also integrated into the resulting polyester chains, leading to the formation of distinct chemical groups. These groups include chain-end-positioned monoester –CH₂OP(O)(OH)₂ observed at approximately 2.5 ppm, inner-chain-positioned diester (–CH₂O)₂P(O)OH at around 1.5 ppm, and branching point triester (–CH₂O)₃P=O at approximately –0.5 ppm (Figure 1). The first two groups may not only act as catalysts due to their acidity, which is comparable to that of H₃PO₄, but may also undergo conversion to –OP(O)(OH)O[–] and (–O)₂P(O)O[–] while being charge-balanced by M²⁺ ions. This conversion process can result in the connection of polymer chains through ionic interactions. The relative abundance of these three units varies depending on several factors such as reaction temperature, the quantity of BHET used in the feed, and the amount of H₃PO₄ added. For example, when preparing the copolyester at a lower temperature of 190 °C using 5.0 mol% BHET and 1.0 mol% H₃PO₄, the copolyester obtained at this conditions being denoted as PBS[5.0T; 1.0P; 190], the mole ratio of monoester/diester/triester, as determined from the intensity of the ³¹P NMR signals, was roughly 17:51:32. However, it is worth noting that these ratios were semi-quantitative due to a significant amount of noise in the baseline, even with extended data-acquisition times. This suggests that the inner-chain-positioned diester is the predominant group under these conditions. As the polycondensation temperature is increased to 200, 210, and 220 °C while keeping the BHET and H₃PO₄ feed amounts constant at 5.0 and 1.0 mol%, respectively, the ratios gradually shift to 13:45:42, 8:44:48, and 0:30:70, respectively (Figure 1a). Namely, at 220 °C, approximately 70% of the initially added H₃PO₄ transforms into the triester group, resulting in polymer chains with long-chain branches, while the remaining 30% forms the inner-chain-positioned diester. When the quantity of BHET in the feed is increased, the contents of monoester and diester units decrease significantly (Figure 1b). For instance, PBS[0T; 1.0P; 210], which does not contain any terephthalate units, exhibits a ratio of 25:58:17 for monoester/diester/triester, indicating substantial amounts of monoester and diester units. However, this ratio decreases to 8:44:48, 4:36:60, and 2:28:70 for PBS[5.0T; 1.0P; 210], PBS[10T; 1.0P; 210], and PBS[15T; 1.0P; 210], respectively, suggesting that chain-end-positioned monoester units are

almost negligible. Notably, the ratios do not show significant changes with an increase in H_3PO_4 feed, remaining relatively constant at 8:44:48, 10:50:40, and 17:51:32 for PBS[5.0T; 1.0P; 210], PBS[5.0T; 2.0P; 210], and PBS[5.0T; 3.0P; 210], respectively (Figure S1).

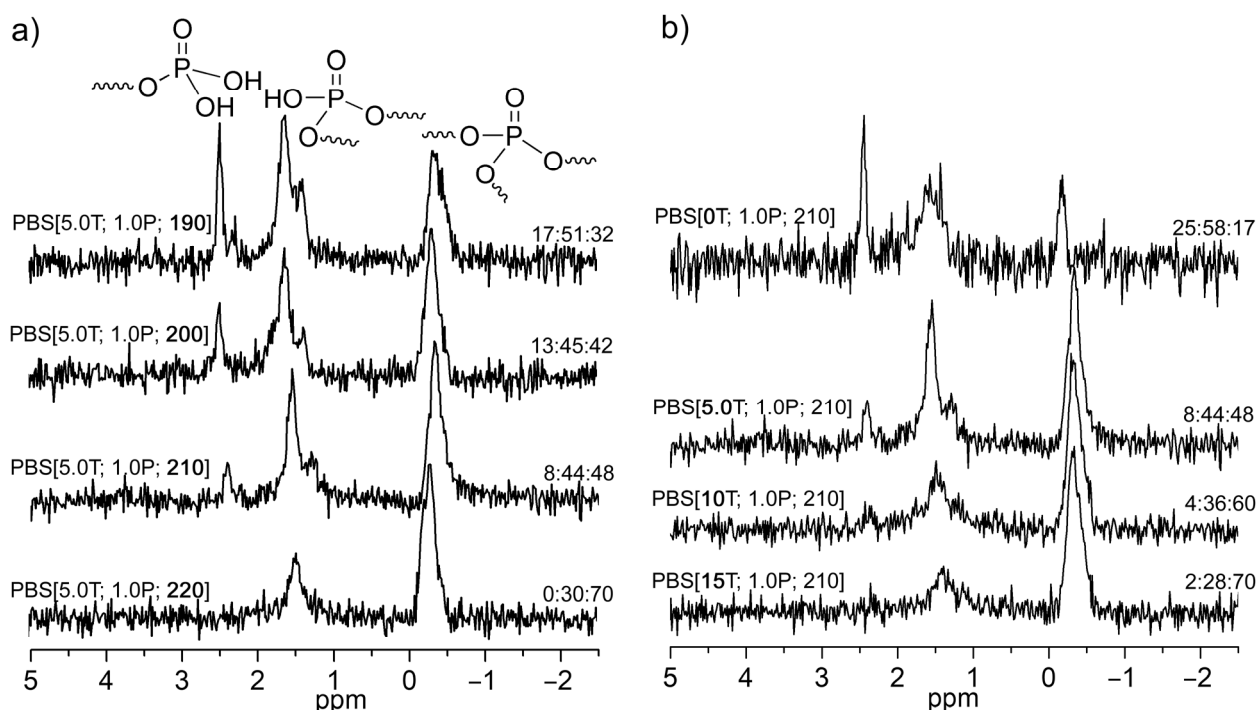


Figure 1. ^{31}P NMR spectra of SA/[BD + 5.0 mol% BHET] copolyesters prepared with (a) variation in temperature (190, 200, 210, and 220 °C) and (b) varying BHET feed quantities (0, 5.0, 10, 15 mol% per SA).

In the 1H NMR spectra of the resulting copolyesters, we observed signals corresponding to terephthalate ($-O_2CC_6H_4CO_2-$, referred to as T) and succinate ($-O_2CCH_2CH_2CO_2-$, referred to as S) at 8.1 and 2.6 ppm, respectively. The intensities of these signals precisely matched the [BHET]/[SA] feed ratio. Additionally, a signal corresponding to the inner CH_2 units in BD (i.e., $-OCH_2CH_2CH_2CH_2O-$) was observed at 1.7 ppm as a prominent signal flanked by two low-intensity signals. However, the signals related to $-CH_2OC(O)-$ were more complex, with a major signal at 4.1 ppm and many low-intensity signals in the downfield region between 4.1 and 4.7 ppm. Importantly, these low-intensity signals were well-resolved, and each of them could be definitively assigned (Figure 2) [67]. Upon completing the signal assignments, it became apparent that nearly all of the $-OCH_2CH_2O-$ units initially present in BHET remained incorporated in the resulting copolyesters, primarily attaching to terephthalate units. For example, the intensity ratio of ([TOCH₂CH₂OT] (referred to as TET, 4.66 ppm) + [TOCH₂CH₂OS] (TES, 4.50 and 4.42 ppm) + [SOCH₂CH₂OS] (SES, 4.25 ppm))/[T] was 1.9 for PBS[5.0T; 1.0P; 210], indicating that 95% of the $-OCH_2CH_2O-$ units initially present in BHET remained incorporated in the copolyester chains as incorporated. Similarly, the intensity ratio of ([TET] + [TES])/([TET] + [TES] + [SES]) was 0.70, suggesting that 70% of the incorporated $-OCH_2CH_2O-$ units remained attached to terephthalate units. These ([TET] + [TES]) + [SES])/[T] ratios consistently fell within the range of 1.8–1.9, and the ([TET] + [TES])/([TET] + [TES] + [SES]) ratios remained steady at 0.64–0.72 throughout all experiments performed with variations in the feed quantity of BHET, H_3PO_4 and temperature (Table 1).

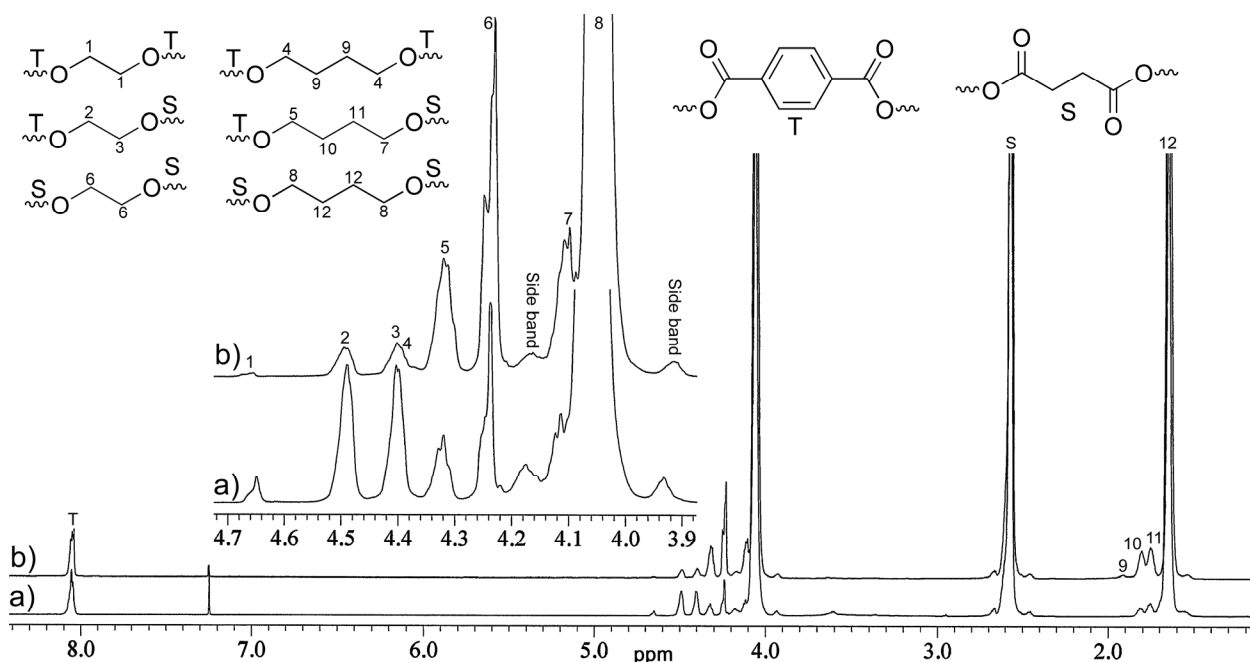


Figure 2. ^1H NMR spectrum of SA/(BD + 5.0 mol% BHET) copolyesters prepared using (a) H_3PO_4 and (b) $(\text{nBuO})_4\text{Ti}$ catalyst. Signal assignments are denoted using the numbers 1–12 and the letters T and S in both the structures and spectra.

Table 1. ^{31}P , ^1H NMR and GPC analysis data for the prepared copolyesters.

Entry	Copolyester ^a	[Monoester]:[Diester]:[Triester] ^b	[TET]:[TES]:[SES]:[TBT]:[TBS]:[SBS] ^c	$M_w; M_w/M_n$ ^d (kDa)
1	[5.0T; 1.0P; 190]	17:52:32	0.24:5.5:2.9:0:3.1:88	33; 2.1
2	[5.0T; 1.0P; 200]	13:45:42	0.27:5.6:2.6:0:3.0:89	45; 2.4
3	[5.0T; 1.0P; 210]	8:44:48	0.34:5.7:2.6:0:2.9:88	44; 2.3
4	[5.0T; 1.0P; 220]	0:30:70	0.36:5.3:3.1:0:3.3:88	81; 3.1
5	[0T; 1.0P; 210]	25:58:17	0:0:0:0:100	77; 2.5
6	[10T; 1.0P; 210]	4:36:60	0.89:11:4.8:0: 5.1:78	62; 2.9
7	[15T; 1.0P; 210]	2:28:70	1.6:16:6.8:0:3.4:72	70; 3.1
8	[20T; 1.0P; 210]	0:30:70	2.4:15:8.1:0:8.1:66	65; 2.8
9	[5.0T; 2.0P; 210]	10:50:40	0.27:5.2:3.1:0:3.5:88	47; 2.5
10	[5.0T; 3.0P; 210]	17:51:32	0.27:5.0:2.9:0:3.2:89	Unfilterable
11	[0T; Ti; 230]		0:0:0:0:100	290; 2.6
12	[5.0T; Ti; 230]		0.081:1.9:7.3:0.27:7.9:83	310; 2.8
13	[10T; Ti; 230]		0.36:4.8:12:0.66:12:71	310; 2.9
14	[15T; Ti; 230]		0.93:8.9:14:0.88:14:62	220; 2.5
15	[20T; Ti; 230]		1.7:12:17:1.7:15:53	200; 2.7

^a [5.0T; 1.0P; 190], for example, indicates the copolyester of PBS prepared using 5.0 mol% BHET per SA and 1.0 mol% H_3PO_4 per SA at a transesterification temperature of 190 °C. ^b The mole ratios of chain-end-positioned monoester $-\text{CH}_2\text{OP}(\text{O})(\text{OH})_2$, inner-chain-positioned diester $(-\text{CH}_2\text{O})_2\text{P}(\text{O})\text{OH}$, and branching-point-triester $(-\text{CH}_2\text{O})_3\text{P}=\text{O}$ units were determined using ^{31}P NMR spectra. ^c [TES] and [TBS] instances represent $-\text{OCH}_2\text{CH}_2\text{O}-$ and $-\text{OCH}_2\text{CH}_2\text{CH}_2\text{CH}_2\text{O}-$ units, respectively, surrounded by terephthalate and succinate, the ratio being determined by ^1H NMR spectra. ^d Molecular weight and dispersity measured using GPC with CHCl_3 as the eluent and polystyrene standards.

A relatively low-molecular-weight copolyester, PBS[5.0T; 1.0P; 190], was obtained with a reasonably narrow molecular-weight distribution at a transesterification temperature of 190 °C ($M_w = 33$ kDa; \mathcal{D} (dispersity) = $M_w/M_n = 2.1$). When the temperature was increased to 200 and 210 °C, the M_w values showed a marginal increase to 45 kDa, along with a slight increase in the \mathcal{D} value to 2.4. However, raising the temperature further to 220 °C resulted in doubling the M_w value to 81 kDa, although the M_n value marginally increased

from 20 to 26 kDa, consequently leading to a substantial increase in the \bar{D} value from 2.4 to 3.1 (Figure S2a). In the ^{31}P NMR spectrum of PBS[5.0T; 1.0P; 220], the monoester $-\text{CH}_2\text{OP}(\text{O})(\text{OH})_2$ units were absent, while the branching-point-triester $(-\text{CH}_2\text{O})_3\text{P}=\text{O}$ units were predominant (70 mol%; Figure 1a). This suggests the formation of copolyester chains containing a substantial number of long-chain branches, which might be the cause of the increase in M_w and \bar{D} values. Increasing the BHET feed quantity also resulted in higher M_w and \bar{D} values, and PBS[5.0T; 1.0P; 210], PBS[10T; 1.0P; 210], and PBS[15T; 1.0P; 210] exhibited M_w values of 44, 62, and 70 kDa, respectively, with \bar{D} values of 2.3, 2.9, and 3.1, respectively (Figure S2b). On the other hand, increasing the H_3PO_4 feed quantity from 1.0 to 2.0 mol% had only a marginal influence on M_w and \bar{D} values, and PBS[5.0T; 1.0P; 210] and PBS[5.0T; 2.0P; 210] showed M_w values of 44 and 47 kDa, respectively, with \bar{D} values of 2.3 and 2.5, respectively (Figure S2c). However, copolyester prepared with 3.0 mol% H_3PO_4 , i.e., PBS[5.0T; 3.0P; 210], was not freely soluble in CHCl_3 , which hindered filtration for GPC analysis. This suggests the possibility of gel formation when a high amount of H_3PO_4 is used.

Analysis of the ^1H NMR spectrum of the volatiles collected during the esterification reaction, conducted with 1.00 mole of SA, 1.00 mole of BD, and 0.050 mole of BHET, revealed the formation of 1.5 moles of H_2O , along with a small amount of THF (11 mmol). This observation suggests that the esterification reaction, which generates H_2O , was not fully completed, with substantial amounts of $-\text{CO}_2\text{H}$ and $-\text{OH}$ groups still remaining, while the formation of the side product THF was minimal (1.1 mol% per BD). The significant formation of THF presented a considerable challenge during the polycondensation of terephthalic acid and BD. For instance, the use of terephthalic acid is not feasible for producing poly(butylene terephthalate) due to the substantial generation of THF. To address this problem, dimethyl terephthalate is employed as an alternative, even though it does not completely eliminate the formation of THF [68]. When attempting esterification using 5.0 mol% dimethyl terephthalate and 10 mol% ethylene glycol as a direct substitute for 5.0 mol% BHET, a significant issue arose in our experiments. Dimethyl terephthalate underwent sublimation, adhering to the walls of the reactor and the glass lines, which led to obstruction of the reaction (Figure S3a). It is worth mentioning that this fouling of the reactor was not encountered when the esterification reaction was conducted using BHET, highlighting the inherent advantage of utilizing BHET over the conventional approach of using terephthalic acid or dimethyl terephthalate (Figure S3b). Indeed, the preparation of copolyesters comprising $-\text{OCH}_2\text{CH}_2\text{CH}_2\text{CH}_2\text{O}-$, $-\text{OCH}_2\text{CH}_2\text{O}-$, succinate, and terephthalate units has been reported [67]. However, it was not directly synthesized using BD, ethylene glycol, SA, and terephthalic acid. Instead, it was prepared from prepolymers of 1,4-butylene succinate, ethylene succinate, and ethylene terephthalate.

The prepared copolyesters, which contained acidic $-\text{CH}_2\text{OP}(\text{O})(\text{OH})_2$ and $(-\text{CH}_2\text{O})_2\text{P}(\text{O})\text{OH}$ groups, exhibited instability and a severe deterioration in their mechanical strength during storage. To address this issue, the copolyesters were treated with divalent metal 2-ethylhexanoate $[(\text{CH}_3(\text{CH}_2)_2\text{CH}(\text{Et})\text{CH}_2\text{CO}_2)_2\text{M}; \text{M} = \text{Mg}, \text{Zn}, \text{Mn}; 1.0 \text{ eq}/\text{H}_3\text{PO}_4]$. It is important to note that divalent Mg, Mn, and Zn ions are essential nutrients in plant growth. Considering the pKa values of the 2-ethylhexanoate anion, $n\text{BuOP}(\text{O})(\text{OH})_2$, and $(n\text{BuO})_2\text{P}(\text{O})(\text{OH})$, which are 4.8, 1.8, and 1.7, respectively, the $-\text{CH}_2\text{OP}(\text{O})(\text{OH})_2$ and $(-\text{CH}_2\text{O})_2\text{P}(\text{O})\text{OH}$ units underwent conversion to $-\text{OP}(\text{O})(\text{OH})\text{O}^-$ and $(-\text{O})_2\text{P}(\text{O})\text{O}^-$ while being charge-balanced by M^{2+} ions upon the addition of the metal 2-ethylhexanoate. This conversion process consequently resulted in the connection of polymer chains through ionic interactions. This conversion process also led to the simultaneous generation of 2-ethylhexanoic acid. Upon the removal of the generated 2-ethylhexanoic acid, the viscosity of the polymer melts significantly increased, leading to a state where the mechanical stirrer in our polymerization setup ceased.

For comparison, we synthesized copolyesters using the conventional method, employing $(n\text{BuO})_4\text{Ti}$ catalyst (200 ppm-Ti/product) and varying the quantities of BHET in the feed (entries 10–13). Surprisingly, under our polymerization conditions and settings,

we achieved significantly high-molecular-weight PBS and copolyesters. Molecular weight (M_w) values of approximately 300 kDa were obtained for feed ratios of 0, 5.0, and 10 mol% BHET per SA, whereas M_w reached 220 kDa for a feed of 15 mol% BHET. The ratios of [TET]:[TES]:[SES]:[TBT]:[TBS]:[SBS] measured in ^1H NMR spectra were notably different from those observed for copolyesters prepared using H_3PO_4 . Extensive transesterification reactions occurred, possibly due to the use of more reactive $(\text{nBuO})_4\text{Ti}$ catalyst or the elevated polymerization temperature of 230 °C. This resulted in the appearance of signals related to TBT units in the ^1H NMR spectra, albeit with relatively low intensities, which were absent in the copolyesters prepared using H_3PO_4 (Figure 2). In addition to this observation, signals associated with TES units decreased while those corresponding to TBS units increased. Consequently, the intensity ratio of $([\text{TET}] + [\text{TES}])/([\text{TET}] + [\text{TES}] + [\text{SES}])$ decreased from 0.64–0.72 to 0.20–0.41 when H_3PO_4 was replaced with $(\text{nBuO})_4\text{Ti}$ catalyst.

3.2. Thermal Properties

In differential scanning calorimetry (DSC) studies, PBS[0T; 1.0P; 210; Mg], which refers to copolyesters obtained by treating PBS[0T; 1.0P; 210] with magnesium 2-ethylhexanoate, exhibited nearly identical thermal properties to PBS[0T; Ti; 230] prepared through the conventional method using $(\text{nBuO})_4\text{Ti}$ catalyst, (T_m (melting temperature), 116 and 114 °C; T_c (crystallization temperature), 68 and 65 °C; T_g (glass transition temperature), –34 and –34 °C, respectively). Usually, thermal properties do not exhibit significant sensitivity to variations in end groups or the attachment of a side group. Upon the incorporation of BHET units (specifically, $-\text{O}_2\text{CC}_6\text{H}_4\text{CO}_2-$ and $-\text{OCH}_2\text{CH}_2\text{O}-$ units), the T_m value decreased to 106 °C for PBS[5.0T; 1.0P; 210; Mg] and further decreased gradually with increasing BHET feed quantities, PBS[10T; 1.0P; 210; Mg] and PBS[15T; 1.0P; 210; Mg] exhibiting T_m signals at 96 and 87 °C, respectively (Figure 3). The copolyester obtained by feeding 20 mol% BHET, i.e., PBS[20T; 1.0P; 210; Mg], showed no T_m signal during its second heating scan, although it exhibited a clear T_m at 77 °C during the first heating scan. This observation suggests that PBS[20T; 1.0P; 210; Mg] is crystalline, but its crystallization rate is significantly slow. The signal intensities, specifically the heat of melting (ΔH), were substantially high for PBS[0T; 1.0P; 210; Mg], PBS[5.0T; 1.0P; 210; Mg], and PBS[10T; 1.0P; 210; Mg], with ΔH values of 61, 55, and 47 J/g, respectively. In contrast, the ΔH value was relatively weak for PBS[15T; 1.0P; 210; Mg], measuring only 18 J/g.

The T_c signals, observed during the cooling process after the first heating scan, were significant at 68 and 48 °C, accompanied by ΔH values of 67 and 55 J/g, for PBS[0T; 1.0P; 210; Mg] and PBS[5.0T; 1.0P; 210; Mg], respectively, while the T_{cc} signals, observed during the second heating process, were feeble. These observations suggest that the crystallization process occurred rapidly for PBS and the copolyester prepared with a small amount of BHET (5 mol%). Interestingly, PBS[10T; 1.0P; 210; Mg] exhibited both T_c and T_{cc} signals at 28 and 19 °C, respectively, with substantial intensities. This indicates the occurrence of the crystallization process at room temperature at a relatively slow pace. In contrast, for PBS[15T; 1.0P; 210; Mg], the T_c signal was not apparent, and it only exhibited a significant T_{cc} signal over a broad temperature range of 20–70 °C, indicating a slow crystallization rate. As for PBS[20T; 1.0P; 210; Mg], neither T_c nor T_{cc} signals were observed.

The thermal properties remained almost unchanged despite variations in polycondensation temperature and the type of metal ions used at the final stage (Table 2, entries 6–8). However, due to a more random distribution of $-\text{O}_2\text{CC}_6\text{H}_4\text{CO}_2-$ and $-\text{OCH}_2\text{CH}_2\text{O}-$ units, copolyesters synthesized with $(\text{nBuO})_4\text{Ti}$ exhibited a more significant reduction in T_m and its associated ΔH value when exposed to the same amount of BHET feed. For example, PBS[5.0T; Ti; 230] and PBS[10T; Ti; 230] displayed T_m signals at 99 and 86 °C, with ΔH values of 47 and 33 J/g, respectively. In contrast, PBS[5.0T; 1.0P; 210; Mg] and PBS[10T; 1.0P; 210; Mg] exhibited T_m signals at 106 and 96 °C, with ΔH values of 55 and 47 J/g, respectively. Both PBS[15T; Ti; 230] and PBS[20T; Ti; 230] did not exhibit any T_m signals during the second heating process. Additionally, PBS[5.0T; Ti; 230] displayed a T_c signal over a broad temperature range of 15–60 °C, while PBS[10T; Ti; 230] only showed a broad

T_{cc} signal at 15–50 °C, without the appearance of a T_c signal. The slow crystallization rate is a significant issue in copolyesters prepared using prepolymers of 1,4-butylene succinate, ethylene succinate, and ethylene terephthalate [67].

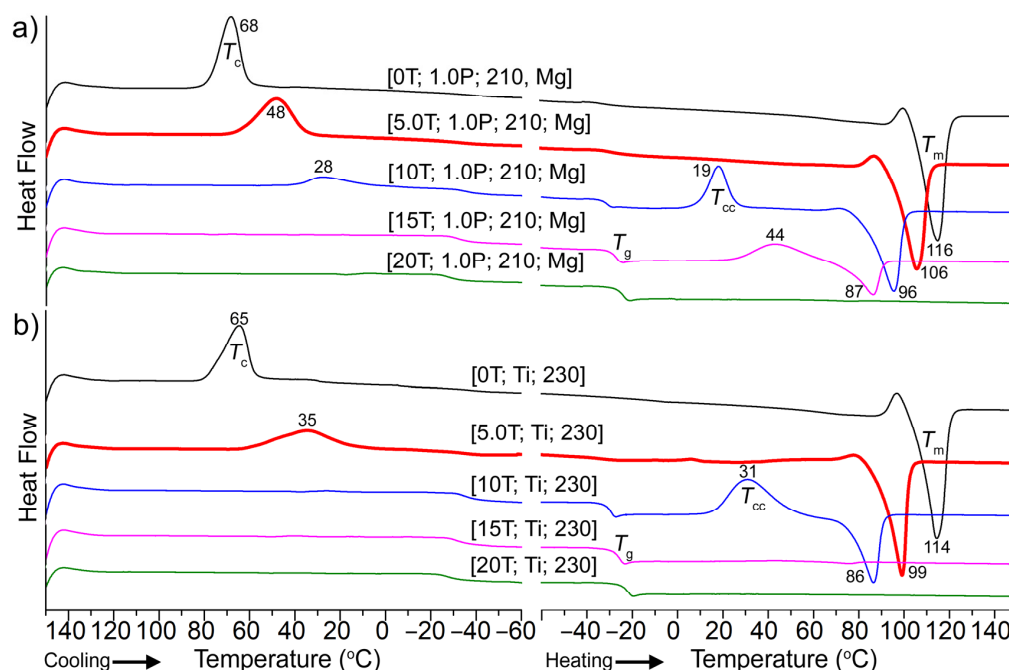


Figure 3. DSC curves for PBS and its copolyesters prepared using (a) $H_3PO_4/Mg(2\text{-ethylhexanoate})_2$ and (b) $(nBuO)_4Ti$ catalyst.

Table 2. Thermal properties of the prepared PBS and its copolyesters prepared using BHET.

Entry	Copolyesters ^a	T_m (°C); ΔH (J/g)	T_c (°C); ΔH (J/g)	T_{cc} (°C); ΔH (J/g)	T_g on DSC (°C)	T_g on DMA (°C) E'_{onset} ; E''_{max} ; $\tan\delta_{max}$
1	[0T; 1.0P; 210; Mg]	116; 61	68; 67	100; 2.4	−34	−30; −20; −14
2	[5.0T; 1.0P; 210; Mg]	106; 55	48; 55	87; 2.8	−28	−23; −16; −9.1
3	[10T; 1.0P; 210; Mg]	96; 47	28; 17	19; 22	−30	−21; −13; −5.3
4	[15T; 1.0P; 210; Mg]	87; 18	n.d.	44; 21	−27	−17; −7.3; 1.0
5	[20T; 1.0P; 210; Mg]	not detected (77) ^b	not detected	not detected	−24	−16; −5.3; 4.0
6	[5.0T; 1.0P; 220; Mg]	106; 53	44; 59	86; 4.8	−29	
7	[5.0T; 1.0P; 210; Zn]	105; 54	43; 56	85; 3.2	−29	
8	[5.0T; 1.0P; 210; Mn]	105; 56	50; 59	86; 3.2	−31	
9	[0T; Ti; 230]	114; 61	65; 60	96; 5.3	−34	−29; −21; −15
10	[5.0T; Ti; 230]	99; 47	35; 47	77; 1.5	−30	−25; −18; −13
11	[10T; Ti; 230]	86; 33	n.d.	31; 39	−31	−23; −16; −9.0
12	[15T; Ti; 230]	n.d. (55–85) ^b	n.d.	n.d.	−27	−20; −12; −4.3
13	[20T; Ti; 230]	n.d. (63) ^b	n.d.	n.d.	−23	−18; −10; −2.0

^a [5.0T; 1.0P; 210; Mg], for example, indicates the copolyester of PBS prepared using 5.0 mol% BHET per SA and 1.0 mol% H_3PO_4 per SA at a transesterification temperature of 210 °C, and finally treated with magnesium 2-ethylhexanoate. ^b T_m signal, as indicated within the parenthesis, was observed during the first heating scan.

The glass transition temperatures (T_g) of PBS[0T; 1.0P; 210; Mg] and PBS[0T; Ti; 230] measured on DSC curves were both −34 °C, and they showed a slight increase upon the incorporation of BHET units, with both PBS[x T; 1.0P; 210; Mg] and PBS[x T; Ti; 230] ($x = 5.0, 10, 15, 20$) series showing T_g signals ranging from −30 °C to −24 °C, with higher T_g values corresponding to a higher BHET content. This same systematic trend was also evident in dynamic mechanical analysis (DMA). The T_g values measured on storage modulus, loss modulus, and $\tan\delta$ curves (i.e., E'_{onset} , E''_{max} , $\tan\delta_{max}$) for PBS[0T; 1.0P; 210; Mg] were −30,

−20, and −14 °C, respectively, which were notably higher than that measured using DSC (−34 °C). These values systematically increased with the increase of BHET content, reaching −16, −5.3, and 4.0 °C, respectively, for PBS[20T; 1.0P; 210; Mg] (Figure 4). A similar trend was also observed for the PBS[*x*T; Ti; 230] (*x* = 0, 5.0, 10, 15, 20) series (Figure S4), although these series displayed slightly lower T_g values compared to their corresponding PBS[*x*T; 1.0P; 210; Mg] counterparts.

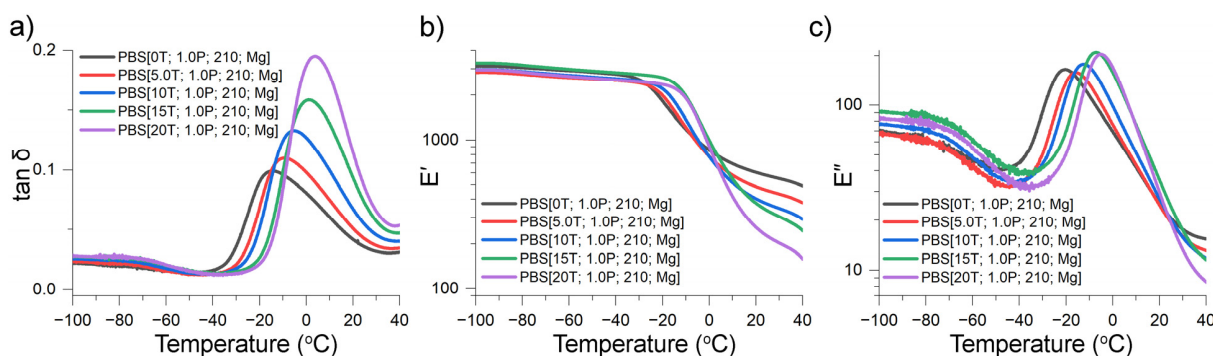


Figure 4. Temperature dependence of (a) $\tan \delta$, (b) storage modulus (E'), (c) loss modulus (E'') curves from DMA runs illustrated for PBS[*x*T; 1.0P; 210; Mg] (*x* = 0, 5.0, 10, 15, 20) series.

The observed thermal properties align well with the wide-angle X-ray diffraction (WAXD) patterns (Figure 5). In both PBS[0T; 1.0P; 210; Mg] and PBS[0T; Ti; 230], we observed fairly sharp and distinct signals at 2θ angles of 19.5, 21.8, and 22.6°. However, these signals became increasingly blurred as BHET units were incorporated into the structure, and the blurring intensified with a higher concentration of BHET units. This blurring effect was marginal in the PBS[*x*T; 1.0P; 210; Mg] series (*x* = 5.0, 10, 15, 20) (Figure 5a). In contrast, the PBS[*x*T; Ti; 230] series exhibited a significant degree of blurring (Figure 5b). This observation was consistent with the ^1H NMR spectra, specifically, a more random distribution of $-\text{O}_2\text{CC}_6\text{H}_4\text{CO}_2-$ and $-\text{OCH}_2\text{CH}_2\text{O}-$ units, and the significant reduction in T_m values observed in the DSC curves for the PBS[*x*T; Ti; 230] series.

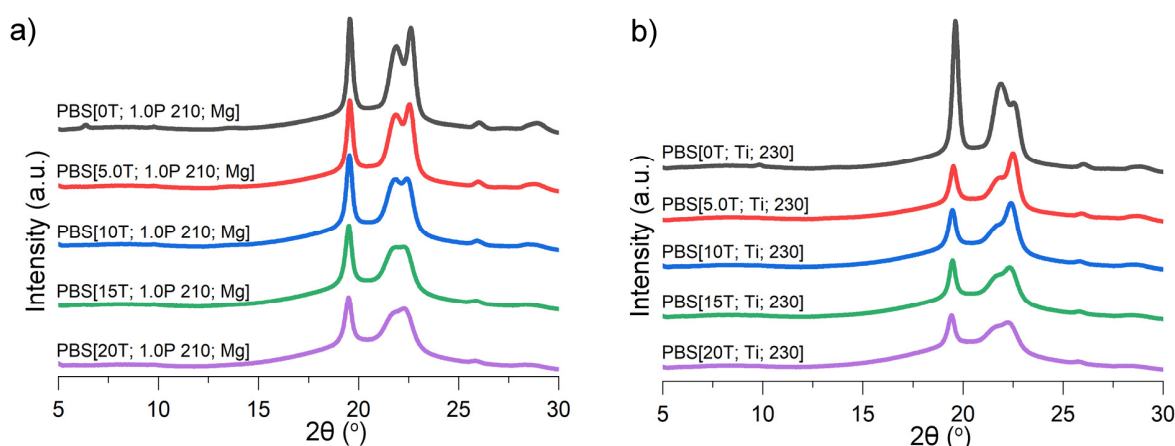


Figure 5. WAXD curves for PBS and its copolyesters prepared using (a) $\text{H}_3\text{PO}_4/\text{Mg}(\text{2-ethylhexanoate})_2$ and (b) $(\text{nBuO})_4\text{Ti}$ catalyst.

3.3. Mechanical Properties

PBS samples with a composition lacking any $-\text{O}_2\text{CC}_6\text{H}_4\text{CO}_2-$ and $-\text{OCH}_2\text{CH}_2\text{O}-$ units demonstrated remarkable tensile strength (34 MPa) and elastic modulus (370 MPa). However, the elongation at break exhibited significant variability among specimens with a substantially high average value of 180 ± 130 . Upon incorporating BHET units, we

observed more consistent tensile data, exhibiting a trend where the yield and ultimate strengths, as well as the elastic modulus, decreased with increasing BHET contents while the elongation at break increased (Figure 6a). The most intriguing sample, PBS[5.0T; 1.0P; 210; Mg], which exhibited a T_m signal at 105 °C and fast crystallization, demonstrated a substantial yield strength (26 MPa) and elastic modulus (290 MPa), along with an impressive elongation at break (370%). Tensile properties displayed a slight deterioration in the case of PBS[5.0T; 1.0P; 200; Mg], which was synthesized at a lower temperature of 200 °C. In contrast, significantly worse tensile properties were observed for PBS[5.0T; 1.0P; 220; Mg], synthesized at a higher temperature of 220 °C (Table 3, entries 7–8; Figure S5a). PBS[5.0T; 2.0P; 210; Mg] and PBS[5.0T; 3.0P; 210; Mg], synthesized with a higher amount of H_3PO_4 , exhibited a brittle character with low elongation at break values of 8% and 16%, respectively, along with reduced tensile strength of 14 MPa (entries 9–10; Figure S5b). Interestingly, the change in metal species did not significantly affect the tensile properties. All three samples, PBS[5.0T; 1.0P; 210; Mg], PBS[5.0T; 1.0P; 210; Zn], and PBS[5.0T; 1.0P; 210; Mn], exhibited similar tensile properties (entries 2 and 11–10; Figure S5c). The role of M^{2+} ions is solely to facilitate the connection of two phosphate groups through ionic interaction, and the mechanical properties are not influenced by the variation in M^{2+} ions. It is important to note that metal ions like Mg, Zn, and Mn are essential plant growth nutrients, though the content of Zn ions in soils is strictly regulated below 300 ppm.

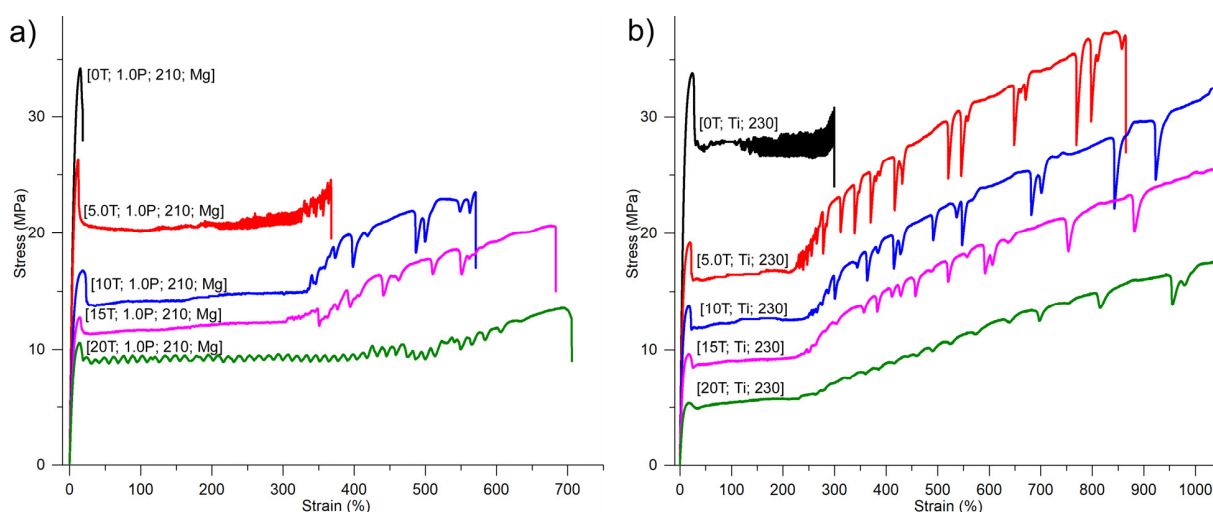


Figure 6. Tensile curves for PBS and its copolyesters prepared using (a) $H_3PO_4/Mg(2\text{-ethylhexanoate})_2$ and (b) $(nBuO)_4Ti$ catalyst.

Table 3. Mechanical properties of the prepared PBS and its copolyesters.

Entry	Copolyesters ^a	Yield Strength σ_y (MPa)	Elastic Modulus E (MPa)	Ultimate Strength σ_u (MPa)	Elongation at Break ϵ (%)
1	[0T; 1.0P; 210; Mg]	34 ± 0.7	370 ± 2	34 ± 0.7	180 ± 130
2	[5.0T; 1.0P; 210; Mg]	26 ± 0.7	290 ± 3	26 ± 0.7	370 ± 30
3	[10T; 1.0P; 210; Mg]	17 ± 0.5	190 ± 6	24 ± 0.4	570 ± 20
4	[15T; 1.0P; 210; Mg]	13 ± 0.4	140 ± 6	21 ± 0.8	680 ± 30
5	[20T; 1.0P; 210; Mg]	10 ± 0.4	110 ± 4	18 ± 0.5	730 ± 40
7	[5.0T; 1.0P; 200; Mg]	24 ± 0.3	270 ± 5	24 ± 0.4	340 ± 30
8	[5.0T; 1.0P; 220; Mg]	22 ± 0.4	240 ± 7	22 ± 0.5	340 ± 80
9	[5.0T; 2.0P; 210; Mg]	14 ± 4	320 ± 40	14 ± 4	8 ± 4
10	[5.0T; 3.0P; 210; Mg]	14 ± 3	250 ± 30	14 ± 3	16 ± 10
11	[5.0T; 1.0P; 210; Zn]	23 ± 0.4	250 ± 5	26 ± 2	430 ± 90
12	[5.0T; 1.0P; 210; Mn]	24 ± 0.2	260 ± 6	25 ± 2	340 ± 50
13	[0T; Ti; 230]	34 ± 1	320 ± 9	34 ± 0.8	300 ± 90

Table 3. Cont.

Entry	Copolyesters ^a	Yield Strength σ_y (MPa)	Elastic Modulus E (MPa)	Ultimate Strength σ_u (MPa)	Elongation at Break ϵ (%)
14	[5.0T; Ti; 230]	19 ± 0.4	200 ± 4	37 ± 2	870 ± 70
15	[10T; Ti; 230]	14 ± 0.4	150 ± 6	Not-broken	Not-broken
16	[15T; Ti; 230]	9.6 ± 0.3	110 ± 4	Not-broken	Not-broken
17	[20T; Ti; 230]	5.4 ± 0.1	58 ± 2	Not-broken	Not-broken

^a [5.0T; 1.0P; 210; Mg], for example, indicates the copolyester of PBS prepared using 5.0 mol% BHET per SA and 1.0 mol% H₃PO₄ per SA at a transesterification temperature of 210 °C, and finally treated with magnesium 2-ethylhexanoate.

PBS[0T; Ti; 230] exhibited a high tensile strength comparable to that of PBS[0T; 1.0P; 210; Mg], although it had a slightly reduced elastic modulus (320 vs. 370 MPa). The elongation at break values showed fluctuations, ranging from 180 to 430%. Upon the incorporation of a small number of BHET units, there was a dramatic improvement in the elongation at break value. PBS[5.0T; Ti; 230] exhibited an elongation at break of 870%, which was significantly higher compared to that of PBS[5.0T; 1.0P; 210; Mg] (870 vs. 370%). However, this improvement came at the expense of reduced yield strength (19 vs. 26 MPa) and a lower elastic modulus (200 vs. 290 MPa). Specimens prepared with PBS[10T; Ti; 230], PBS[15T; Ti; 230], and PBS[20T; Ti; 230] were strong and unbroken, even at the instrument's ultimate elongation of 1000% (Figure 6b). The yield strength and elastic modulus gradually decreased with the increasing BHET contents. Interestingly, the latter two samples did not exhibit T_m signals in the second heating scans, but slowly crystallized at room temperature, resulting in initially transparent specimens turning hazy. Tensile properties were measured after this crystallization process.

3.4. Rheological Properties

Usually, polymers exhibit shear-thinning behavior in rheology, which means that their viscosity decreases under shear strain. This behavior deviates from Newtonian flow, where viscosity remains constant, regardless of shear strain. Due to the presence of long-chain branches, either through phosphate triester linkages [(-CH₂O)₃P=O] or through diester linkages via ionic bonds [(-CH₂O)₂P(O)(O⁻)Mg²⁺(O⁻)P(O)], the PBS[*x*T; 1.0P; 210, Mg] (*x* = 0, 5.0, 10, 15, 20) series exhibited significant shear-thinning behavior in the flow curves measured using a rotational rheometer at 170 °C. Specifically, the complex viscosities (η^*) of the ionic aggregates PBS[*x*T; 1.0P; 210, Mg] at a low angular frequency of 0.1 rad/s were notably high and varied among the samples, ranging from 8600 to 89000 Pa·s. These values were much higher than the η^* value of 5400 Pa·s measured for a commercial PBAT sample with a M_w of 230 kDa and a D of 4.4. As the angular frequency increased, the η^* values significantly decreased, with all samples, including PBAT, exhibiting a similar low viscosity level of 250–540 Pa·s at a high angular frequency of 630 rad/s (Figure 7a). This remarkable sensitivity of viscosity to angular frequency is known to be a crucial advantage in various melt processing applications such as blowing and casting films, injection and blow molding, and thermoforming [69,70]. In contrast, the conventional PBSs (PBS[*x*T; Ti; 230]) prepared using conventional methods with the (nBuO)₄Ti catalyst and lacking long-chain branches did not display such prominent shear-thinning behavior. These conventional PBSs exhibited relatively low η^* values of 4100–9500 Pa·s at a low angular frequency of 0.1 rad/s, while at a high angular frequency of 630 rad/s, they showed similar η^* values ranging from 510 to 670 Pa·s (Figure 7b).

The cross-over point observed in the storage-modulus and loss-modulus curves measured using a rotational rheometer is correlated with molecular weight and dispersity. Specifically, a lower angular frequency at the crossover point corresponds to a higher molecular weight, while a lower modulus at the crossover point indicates a wider dispersity [71]. In the case of ionic aggregates, such as those prepared in this study by reacting copolyesters containing -CH₂OP(O)(OH)₂ and (-CH₂O)₂P(O)OH groups with divalent

metal 2-ethylhexanoate, it is impossible to measure their molecular weights using GPC analysis. Therefore, estimating their molecular weights and dispersity qualitatively through the crossover points becomes a meaningful approach. For the PBS[*x*T; 1.0P; 210, Mg] (*x* = 0, 5.0, 10, 15, 20) series, these ionic aggregates exhibited crossover points at much lower angular frequencies and lower moduli compared to conventional PBSs (i.e., PBS[*x*T; Ti; 230] series) prepared using conventional methods with (nBuO)₄Ti catalyst (2–25 vs. 160–320 rad/s; 25–39 vs. 150–170 kPa; Figures 8 and S6). The data suggest that the ionic aggregates, formed by connecting low-molecular-weight chains (*M_w* = 44 kDa) with divalent metal ions, behave in the molten state as if they were much higher molecular weight polymers than the conventional ones, which already had significantly high molecular weights according to GPC analysis (*M_w* = 200–300 kDa). Furthermore, these findings indicate that the dispersity values of the ionic aggregates are much broader than those of conventional PBS, which aligns with their higher shear-thinning behavior due to the presence of long-chain branches.

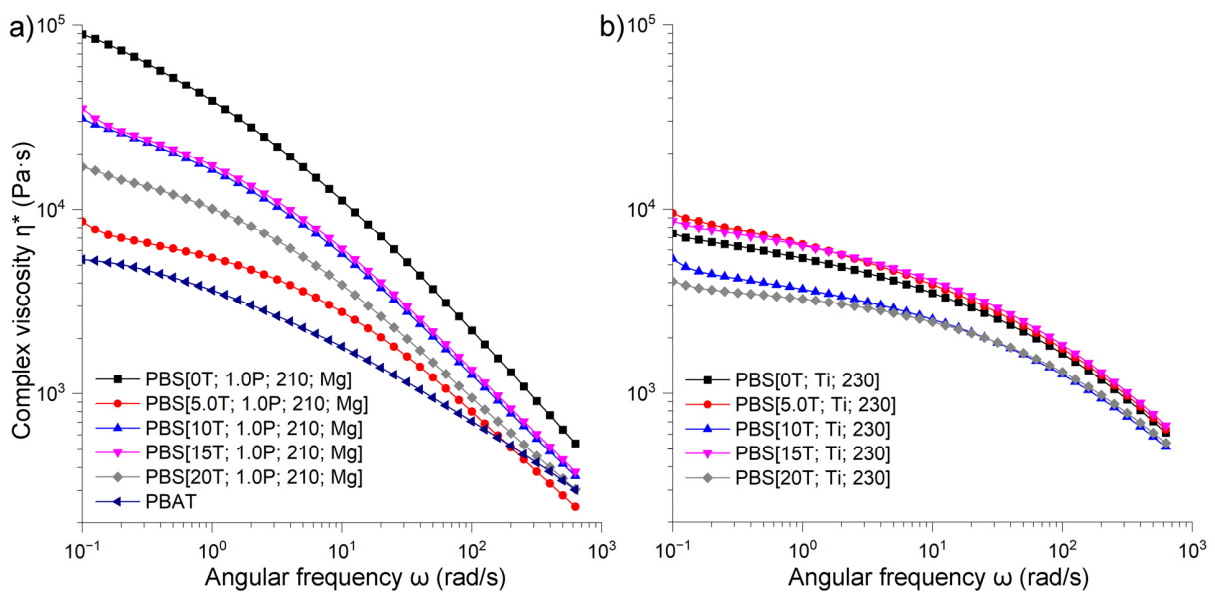


Figure 7. Flow curves measured using rotational rheometer at 170 °C for PBS and its copolyesters prepared using (a) H₃PO₄/Mg(2-ethylhexanoate)₂ and (b) (nBuO)₄Ti catalyst.

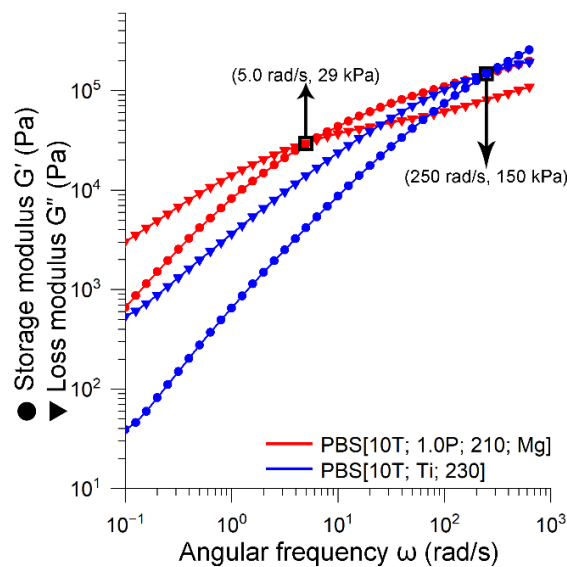


Figure 8. Comparison of dynamic moduli vs. angular frequency between PBS[10T; 1.0P; 210, Mg] and PBS[10T; Ti; 230].

3.5. Biodegradability

Like PLA, PBS is known to exhibit resistance to degradation under ambient conditions in soil, marine environments, and freshwater, only undergoing composting in harsh industrial composting settings with temperatures reaching 60 °C and an abundance of microbiomes [2]. In a previous study, we investigated the biodegradability of ionic aggregates of PBAT, which demonstrated a significant enhancement in biodegradability when compared to conventional PBAT under ambient soil conditions [58]. Upon that information, biodegradability of the ionic aggregates of PBS (specifically, PBS[5.0T; 1.0P; 210, M], M = Zn, Mg, Mn) were evaluated. Biodegradability assessments were conducted in an ECHO[®] respirometer (ECHO Instruments, Slovenske Konjice, Slovenia), in accordance with ISO 17556 [66] guidelines, ensuring a constant temperature of 25 °C and a humidity level between 50 and 55%. CO₂ evolution was continuously monitored under a controlled airflow. During the 110-day incubation period, the ionic aggregates of PBS, containing the same amount of M²⁺, -CH₂OP(O)(OH)O⁻, (-CH₂O)₂P(O)O⁻ groups as in the ionic aggregates of PBAT, did not display a significant improvement in biodegradability. This was evident, as the total CO₂ evolved from PBS was considerably lower compared to microcrystalline cellulose (Figure 9). The different biodegradability behaviors observed between PBS and PBAT cannot be easily explained. However, it is worth noting that PBAT is known to exhibit superior biodegradability compared to PBS or PLA; certain grades of PBAT obtained certification for biodegradability under ambient soil conditions, whereas the latter two only achieve certification under artificial industrial composting conditions at 58 °C [2]. It is important to recognize that the market's demand is not necessarily for rapidly biodegradable polymers. What the market seeks are polymers that remain persistent for a certain period during use and subsequently undergo rapid biodegradation.

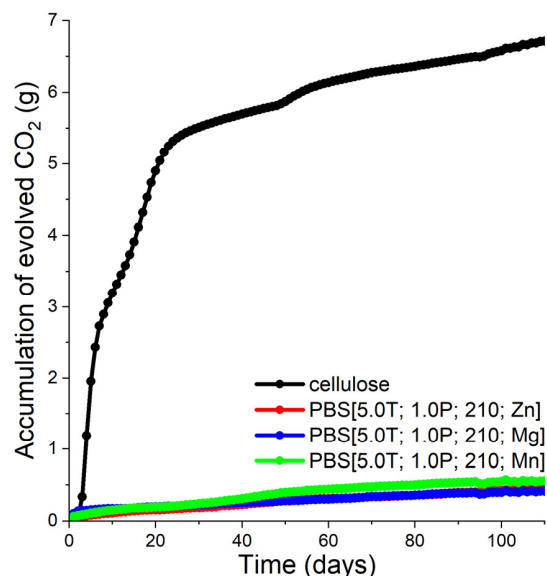


Figure 9. Biodegradability assessments of PBS[5.0T; 1.0P; 210, M] (M = Zn, Mg, Mn) compared to microcrystalline cellulose monitored by measuring evolved CO₂ over time in a respirometer set to 25 °C and 50–55% humidity.

4. Conclusions

A range of PBS-based copolyesters with varying BHET content (5–20 mol% BHET units), specifically containing -O₂CC₆H₄CO₂- and -OCH₂CH₂O- units, were synthesized by SA/[BD + BHET] polycondensation with either 1–3 mol% H₃PO₄ or the conventional (nBuO)₄Ti catalyst. The copolyesters produced using H₃PO₄ (PBS[xT; yP; T] series) contained chain-end-positioned monoester (-CH₂OP(O)(OH)₂), inner-chain-positioned diester (-CH₂O)₂P(O)OH, and branching-point-triester (-CH₂O)₃P=O groups. The relative abundance of these groups varied based on reaction temperature and the amount of BHET in

the feed. Analysis of ^1H NMR spectra indicated that $-\text{O}_2\text{CC}_6\text{H}_4\text{CO}_2-$ and $-\text{OCH}_2\text{CH}_2\text{O}-$ units were distributed more randomly in the copolyesters prepared using the $(\text{nBuO})_4\text{Ti}$ catalyst. The $\text{PBS}[x\text{T}; y\text{P}; T]$ series were treated with $\text{M}(2\text{-ethylhexanoate})_2$ ($\text{M} = \text{Mg}, \text{Zn}, \text{Mn}$) in the final stage to create ionic aggregates, $\text{PBS}[x\text{T}; y\text{P}; T; \text{M}]$ series. These aggregates featured polymer chains extended through ionic bonds between divalent metal cations and $-\text{CH}_2\text{OP}(\text{O})(\text{OH})\text{O}^-$ or $(-\text{CH}_2\text{O})_2\text{P}(\text{O})\text{O}^-$ anions. DSC studies revealed that the T_m values gradually decreased with increasing BHET content, with a more significant reduction observed in copolyesters prepared using the $(\text{nBuO})_4\text{Ti}$ catalyst. Specifically, the copolyester containing 5 mol% BHET units, prepared using $\text{H}_3\text{PO}_4/\text{Mg}(2\text{-ethylhexanoate})_2$ and $(\text{nBuO})_4\text{Ti}$ catalyst, exhibited T_m values of 105 and 99 °C, respectively. Crystallization rates were also reduced with the addition of BHET units, and only PBS and its copolyesters containing 5 mol% BHET units displayed crystallization signals (T_c) during the cooling scan. Incorporation and increase in BHET units led to a gradual decrease in tensile strength and elastic modulus, while elongation at break increased. Notably, $\text{PBS}[5.0\text{T}; 1.0\text{P}; 210; \text{Mg}]$ exhibited impressive mechanical properties with a substantial yield strength (26 MPa) and elastic modulus (290 MPa), along with an elongation at break of 370%. In contrast, its corresponding copolyesters prepared using the $(\text{nBuO})_4\text{Ti}$ catalyst, $\text{PBS}[5.0\text{T}; \text{Ti}; 230]$, displayed a much higher elongation at break of 870%, albeit at the expense of reduced yield strength (19 MPa) and elastic modulus (200 MPa). Due to the presence of long-chain branches, the copolyesters prepared with $\text{H}_3\text{PO}_4/\text{Mg}(2\text{-ethylhexanoate})_2$ exhibited significant shear-thinning behavior in the flow curves, while the copolyesters prepared using $(\text{nBuO})_4\text{Ti}$ catalysts did not exhibit such prominent shear-thinning behavior. Disappointingly, the ionic aggregates of $\text{PBS}[5.0\text{T}; 1.0\text{P}; 210; \text{M}]$ ($\text{M} = \text{Mg}, \text{Zn}, \text{Mn}$) did not display any significant enhancement in biodegradability, in contrast to the rapid biodegradation observed with the ionic aggregates of PBAT.

5. Patents

A patent was applied (Kr 10-2023-0175717, 6 December 2023, assigned to Ajou University).

Supplementary Materials: The following supporting information can be downloaded at: <https://www.mdpi.com/article/10.3390/polym16040519/s1>, Figure S1: ^{31}P NMR spectra; Figure S2: GPC curves. Figure S3: Images illustrating reactor fouling; Figure S4: DMA curves; Figure S5: Tensile curves; Figure S6: Dynamic moduli vs. angular frequency.

Author Contributions: B.Y.L. and P.C.L. conceived the idea, guided the project, and wrote the manuscript. S.U.P. and H.J.S. synthesized polymers. Y.H.S., J.Y.P. and H.K. characterized polymers. W.Y.C. performed the biodegradability studies. All authors have read and agreed to the published version of the manuscript.

Funding: This research was supported by the National Research Foundation of Korea (Grant Number 2020M3A9I5037889) by the Korea Institute of Marine Science and Technology Promotion (KIMST) funded by the Ministry of Oceans and Fisheries (20220258).

Institutional Review Board Statement: Not applicable.

Data Availability Statement: All data are included in this article and in the Supplementary Materials.

Conflicts of Interest: The authors declare no conflicts of interest.

References

1. Fagnani, D.E.; Tami, J.L.; Copley, G.; Clemons, M.N.; Getzler, Y.D.Y.L.; McNeil, A.J. 100th Anniversary of Macromolecular Science Viewpoint: Redefining Sustainable Polymers. *ACS Macro Lett.* **2021**, *10*, 41–53. [[CrossRef](#)]
2. Skoczinski, P.; Krause, L.; Raschka, A.; Dammer, L.; Carus, M. Chapter One—Current status and future development of plastics: Solutions for a circular economy and limitations of environmental degradation. In *Methods in Enzymology*; Weber, G., Bornscheuer, U.T., Wei, R., Eds.; Academic Press: Cambridge, MA, USA, 2021; Volume 648, pp. 1–26.
3. Chen, X.; Cheng, L.; Gu, J.; Yuan, H.; Chen, Y. Chemical recycling of plastic wastes via homogeneous catalysis: A review. *Chem. Eng. J.* **2024**, *479*, 147853. [[CrossRef](#)]
4. Li, A.; Sheng, Y.; Cui, H.; Wang, M.; Wu, L.; Song, Y.; Yang, R.; Li, X.; Huang, H. Discovery and mechanism-guided engineering of BHET hydrolases for improved PET recycling and upcycling. *Nat. Commun.* **2023**, *14*, 4169. [[CrossRef](#)]

5. Zhao, Y.; Rettner, E.M.; Harry, K.L.; Hu, Z.; Miscall, J.; Rorrer, N.A.; Miyake, G.M. Chemically recyclable polyolefin-like multiblock polymers. *Science* **2023**, *382*, 310–314. [[CrossRef](#)] [[PubMed](#)]
6. Zou, L.; Xu, R.; Wang, H.; Wang, Z.; Sun, Y.; Li, M. Chemical recycling of polyolefins: A closed-loop cycle of waste to olefins. *Natl. Sci. Rev.* **2023**, *10*, nwad207. [[CrossRef](#)] [[PubMed](#)]
7. Hassanian-Moghaddam, D.; Asghari, N.; Ahmadi, M. Circular Polyolefins: Advances toward a Sustainable Future. *Macromolecules* **2023**, *56*, 5679–5697. [[CrossRef](#)]
8. Gallin, C.F.; Lee, W.W.; Byers, J.A. A Simple, Selective, and General Catalyst for Ring Closing Depolymerization of Polyesters and Polycarbonates for Chemical Recycling. *Angew. Chem.-Int. Ed.* **2023**, *62*, e202303762. [[CrossRef](#)] [[PubMed](#)]
9. Jung, H.; Shin, G.; Kwak, H.; Hao, L.T.; Jegal, J.; Kim, H.J.; Jeon, H.; Park, J.; Oh, D.X. Review of polymer technologies for improving the recycling and upcycling efficiency of plastic waste. *Chemosphere* **2023**, *320*, 138089. [[CrossRef](#)] [[PubMed](#)]
10. Li, X.; Zheng, G.; Li, Z.; Fu, P. Formulation, performance and environmental/agricultural benefit analysis of biomass-based biodegradable mulch films: A review. *Eur. Polym. J.* **2024**, *203*, 112663. [[CrossRef](#)]
11. Marasović, P.; Kopitar, D.; Brunšek, R.; Schwarz, I. Performance and Degradation of Nonwoven Mulches Made of Natural Fibres and PLA Polymer—Open Field Study. *Polymers* **2023**, *15*, 4447. [[CrossRef](#)] [[PubMed](#)]
12. Li, Y.; Liu, C.; Wei, H.; Gai, X.; Lei, T.; Wang, Y.; Li, Q.; Xiao, H. Recent Advances of Biodegradable Agricultural Mulches from Renewable Resources. *ACS Sustain. Chem. Eng.* **2023**, *11*, 14866–14885. [[CrossRef](#)]
13. Choi, S.Y.; Lee, Y.; Yu, H.E.; Cho, I.J.; Kang, M.; Lee, S.Y. Sustainable production and degradation of plastics using microbes. *Nat. Microbiol.* **2023**, *8*, 2253–2276. [[CrossRef](#)] [[PubMed](#)]
14. Kim, M.S.; Chang, H.; Zheng, L.; Yan, Q.; Pflieger, B.F.; Klier, J.; Nelson, K.; Majumder, E.L.; Huber, G.W. A Review of Biodegradable Plastics: Chemistry, Applications, Properties, and Future Research Needs. *Chem. Rev.* **2023**, *123*, 9915–9939. [[CrossRef](#)]
15. Nelson, T.F.; Rothauer, D.; Sander, M.; Mecking, S. Degradable and Recyclable Polyesters from Multiple Chain Length Bio- and Waste-Sourceable Monomers. *Angew. Chem.-Int. Ed.* **2023**, *62*, e202310729. [[CrossRef](#)]
16. Li, J.; Wang, D.; Jin, J.; Li, F.; Gao, Y.; Liang, H.; Jiang, W. Improving the Shear and Tack Strengths of Chlorinated Poly(propylene carbonate) through Chain Extension with Poly(lactic acid) for Biodegradable Hot Melt Adhesives. *ACS Appl. Polym. Mater.* **2023**, *5*, 10256–10264. [[CrossRef](#)]
17. Zhang, Z.; Quinn, E.C.; Olmedo-Martínez, J.L.; Caputo, M.R.; Franklin, K.A.; Müller, A.J.; Chen, E.Y.X. Toughening Brittle Bio-P3HB with Synthetic P3HB of Engineered Stereomicrostructures. *Angew. Chem.-Int. Ed.* **2023**, *62*, e202311264. [[CrossRef](#)]
18. Erceg, T.; Rackov, S.; Terek, P.; Pilić, B. Preparation and Characterization of PHBV/PCL-Diol Blend Films. *Polymers* **2023**, *15*, 4694. [[CrossRef](#)]
19. Fortună, M.E.; Ungureanu, E.; Rotaru, R.; Barga, A.; Ungureanu, O.C.; Brezuleanu, C.O.; Harabagiu, V. Synthesis and Properties of Modified Biodegradable Polymers Based on Caprolactone. *Polymers* **2023**, *15*, 4731. [[CrossRef](#)]
20. Lackner, M.; Mukherjee, A.; Koller, M. What Are “Bioplastics”? Defining Renewability, Biosynthesis, Biodegradability, and Biocompatibility. *Polymers* **2023**, *15*, 4695. [[CrossRef](#)]
21. Tubio, C.R.; Valle, X.; Carvalho, E.; Moreira, J.; Costa, P.; Correia, D.M.; Lanceros-Mendez, S. Poly(3-hydroxybutyrate-co-3-hydroxyvalerate) Blends with Poly(caprolactone) and Poly(lactic acid): A Comparative Study. *Polymers* **2023**, *15*, 4566. [[CrossRef](#)]
22. Jiang, B.; Wang, Y.; Peng, Z.; Lim, K.H.; Wang, Q.; Shi, S.; Zheng, J.; Yang, X.; Liu, P.; Wang, W.J. Synthesis of Poly(butylene adipate terephthalate)-co-poly(glycolic acid) with Enhanced Degradability in Water. *Macromolecules* **2023**, *56*, 9207–9217. [[CrossRef](#)]
23. Mai, J.; Garvey, C.J.; Chan, C.M.; Pratt, S.; Laycock, B. Synthesis and characterisation of poly(3-hydroxybutyrate-co-3-hydroxyvalerate) (PHBV) multi-block copolymers comprising blocks of differing 3-hydroxyvalerate contents. *Chem. Eng. J.* **2023**, *475*, 146175. [[CrossRef](#)]
24. Qu, D.; Yang, Z.; Zhang, J.; Wang, S.; Lu, Y. Brief Analysis on the Degradation of Sugar-Based Copolyesters. *Polymers* **2023**, *15*, 4372. [[CrossRef](#)]
25. Little, A.; Ma, S.; Haddleton, D.M.; Tan, B.; Sun, Z.; Wan, C. Synthesis and Characterization of High Glycolic Acid Content Poly(glycolic acid-co-butylene adipate-co-butylene terephthalate) and Poly(glycolic acid-co-butylene succinate) Copolymers with Improved Elasticity. *ACS Omega* **2023**, *8*, 38658–38667. [[CrossRef](#)]
26. Saller, K.M.; Hubner, G.; Schwarzing, C. Introducing free carboxylic acid groups along polyester chains using dimethylolpropionic acid as diol component. *Eur. Polym. J.* **2023**, *198*, 112442. [[CrossRef](#)]
27. Zheng, L.; Kim, M.S.; Xu, S.; Urgan-Demirtas, M.; Huber, G.W.; Klier, J. Biodegradable High-Molecular-Weight Poly(pentylene adipate-co-terephthalate): Synthesis, Thermo-Mechanical Properties, Microstructures, and Biodegradation. *ACS Sustain. Chem. Eng.* **2023**, *11*, 13885–13895. [[CrossRef](#)]
28. Hwang, D.K.; Chung, S.; Kim, S.; Park, J.; Ryu, J.; Park, J.; Oh, D.X.; Jeon, H.; Koo, J.M. Exploring the potential of 2,5-furandicarboxylic acid-based bioplastics: Properties, synthesis, and applications. *Polym. Degrad. Stab.* **2023**, *218*, 110539. [[CrossRef](#)]
29. Kanwal, A.; Zhang, M.; Sharaf, F.; Li, C. Polymer pollution and its solutions with special emphasis on Poly (butylene adipate terephthalate) (PBAT). *Polym. Bull.* **2022**, *79*, 9303–9330. [[CrossRef](#)]
30. Yu, J.; Xu, S.; Liu, B.; Wang, H.; Qiao, F.; Ren, X.; Wei, Q. PLA bioplastic production: From monomer to the polymer. *Eur. Polym. J.* **2023**, *193*, 112076. [[CrossRef](#)]
31. Rafiqah, S.A.; Khalina, A.; Harmaen, A.S.; Tawakkal, I.A.; Zaman, K.; Asim, M.; Nurrazi, M.N.; Lee, C.H. A Review on Properties and Application of Bio-Based Poly(Butylene Succinate). *Polymers* **2021**, *13*, 1436. [[CrossRef](#)] [[PubMed](#)]

32. Aliotta, L.; Seggiani, M.; Lazzeri, A.; Gigante, V.; Cinelli, P. A Brief Review of Poly (Butylene Succinate) (PBS) and Its Main Copolymers: Synthesis, Blends, Composites, Biodegradability, and Applications. *Polymers* **2022**, *14*, 844. [[CrossRef](#)]
33. Kim, H.; Shin, G.; Jang, M.; Nilsson, F.; Hakkarainen, M.; Kim, H.J.; Hwang, S.Y.; Lee, J.; Park, S.B.; Park, J.; et al. Toward Sustaining Bioplastics: Add a Pinch of Seasoning. *ACS Sustain. Chem. Eng.* **2023**, *11*, 1846–1856. [[CrossRef](#)]
34. Kindler, A.; Zelder, O. Biotechnological and Chemical Production of Monomers from Renewable Raw Materials. In *Advances in Polymer Science*; Springer: Cham, Switzerland, 2024; Volume 293, pp. 1–33.
35. Yang, Y.; Zhao, J.; Zhou, Y.; Xu, S.; Ren, X.; Wei, Q. Progress on production of succinic acid by *Actinobacillus succinogenes*—New opportunities for cheap biomass and waste gas utilization. *J. Clean. Prod.* **2024**, *434*, 140005. [[CrossRef](#)]
36. Kim, J.Y.; Lee, J.A.; Lee, S.Y. Biobased Production of Succinic Acid and Its Derivatives Using Metabolically Engineered Microorganisms. *Ind. Biotechnol.* **2023**, *19*, 125–137. [[CrossRef](#)]
37. Kim, J.Y.; Ahn, Y.J.; Lee, J.A.; Lee, S.Y. Recent advances in the production of platform chemicals using metabolically engineered microorganisms. *Curr. Opin. Green Sustain. Chem.* **2023**, *40*, 100777. [[CrossRef](#)]
38. Hu, X.; Su, T.; Pan, W.; Li, P.; Wang, Z. Difference in solid-state properties and enzymatic degradation of three kinds of poly(butylene succinate)/cellulose blends. *RSC Adv.* **2017**, *7*, 35496–35503. [[CrossRef](#)]
39. Chae, H.G.; Park, S.H.; Kim, B.C.; Kim, D.K. Effect of methyl substitution of the ethylene unit on the physical properties of poly(butylene succinate). *J. Polym. Sci. Part B Polym. Phys.* **2004**, *42*, 1759–1766. [[CrossRef](#)]
40. Nagata, M.; Goto, H.; Sakai, W.; Tsutsumi, N. Synthesis and enzymatic degradation of poly(tetramethylene succinate) copolymers with terephthalic acid. *Polymer* **2000**, *41*, 4373–4376. [[CrossRef](#)]
41. Cao, A.; Okamura, T.; Nakayama, K.; Inoue, Y.; Masuda, T. Studies on syntheses and physical properties of biodegradable aliphatic poly(butylene succinate-co-ethylene succinate)s and poly(butylene succinate-co-diethylene glycol succinate)s. *Polym. Degrad. Stab.* **2002**, *78*, 107–117. [[CrossRef](#)]
42. Kim, T.; Jeon, H.; Jegal, J.; Kim, J.H.; Yang, H.; Park, J.; Oh, D.X.; Hwang, S.Y. Trans crystallization behavior and strong reinforcement effect of cellulose nanocrystals on reinforced poly(butylene succinate) nanocomposites. *RSC Adv.* **2018**, *8*, 15389–15398. [[CrossRef](#)]
43. Nikolic, M.S.; Djonlagic, J. Synthesis and characterization of biodegradable poly(butylene succinate-co-butylene adipate)s. *Polym. Degrad. Stab.* **2001**, *74*, 263–270. [[CrossRef](#)]
44. Pérez-Camargo, R.A.; Fernández-d’Arlas, B.; Cavallo, D.; Debuissy, T.; Pollet, E.; Avérous, L.; Müller, A.J. Tailoring the Structure, Morphology, and Crystallization of Isodimorphic Poly(butylene succinate-ran-butylene adipate) Random Copolymers by Changing Composition and Thermal History. *Macromolecules* **2017**, *50*, 597–608. [[CrossRef](#)]
45. Luo, S.; Li, F.; Yu, J.; Cao, A. Synthesis of poly(butylene succinate-co-butylene terephthalate) (PBST) copolyesters with high molecular weights via direct esterification and polycondensation. *J. Appl. Polym. Sci.* **2010**, *115*, 2203–2211. [[CrossRef](#)]
46. Li, F.; Xu, X.; Li, Q.; Li, Y.; Zhang, H.; Yu, J.; Cao, A. Thermal degradation and their kinetics of biodegradable poly(butylene succinate-co-butylene terephthalate)s under nitrogen and air atmospheres. *Polym. Degrad. Stab.* **2006**, *91*, 1685–1693. [[CrossRef](#)]
47. Wu, L.; Mincheva, R.; Xu, Y.; Raquez, J.-M.; Dubois, P. High Molecular Weight Poly(butylene succinate-co-butylene furandicarboxylate) Copolyesters: From Catalyzed Polycondensation Reaction to Thermomechanical Properties. *Biomacromolecules* **2012**, *13*, 2973–2981. [[CrossRef](#)] [[PubMed](#)]
48. Mochizuki, M.; Mukai, K.; Yamada, K.; Ichise, N.; Murase, S.; Iwaya, Y. Structural Effects upon Enzymatic Hydrolysis of Poly(butylene succinate-co-ethylene succinate)s. *Macromolecules* **1997**, *30*, 7403–7407. [[CrossRef](#)]
49. Safari, M.; Otaegi, I.; Aramburu, N.; Guerrica-Echevarria, G.; de Ilarduya, A.M.; Sardon, H.; Müller, A.J. Synthesis, Structure, Crystallization and Mechanical Properties of Isodimorphic PBS-ran-PCL Copolyesters. *Polymers* **2021**, *13*, 2263. [[CrossRef](#)] [[PubMed](#)]
50. Park, S.S.; Chae, S.H.; Im, S.S. Transesterification and crystallization behavior of poly(butylene succinate)/poly(butylene terephthalate) block copolymers. *J. Polym. Sci. Part A Polym. Chem.* **1998**, *36*, 147–156. [[CrossRef](#)]
51. Zhou, T.; Wang, B.; Wang, X.; Sun, H.; Liu, Y.; Zheng, L. Copolymers Based on PBS and Polydimethylsiloxane with Improved Properties and Novel Functions: Effect of Molecular Weight of Polydimethylsiloxane. *ACS Sustain. Chem. Eng.* **2023**, *11*, 15397–15409. [[CrossRef](#)]
52. Bautista, M.; Martínez de Ilarduya, A.; Alla, A.; Vives, M.; Morató, J.; Muñoz-Guerra, S. Cationic poly(butylene succinate) copolyesters. *Eur. Polym. J.* **2016**, *75*, 329–342. [[CrossRef](#)]
53. Jacquiel, N.; Freyermouth, F.; Fenouillot, F.; Rousseau, A.; Pascault, J.P.; Fuertes, P.; Saint-Loup, R. Synthesis and properties of poly(butylene succinate): Efficiency of different transesterification catalysts. *J. Polym. Sci. Part A Polym. Chem.* **2011**, *49*, 5301–5312. [[CrossRef](#)]
54. Sugihara, S.; Toshima, K.; Matsumura, S. New Strategy for Enzymatic Synthesis of High-Molecular-Weight Poly(butylene succinate) via Cyclic Oligomers. *Macromol. Rapid Commun.* **2006**, *27*, 203–207. [[CrossRef](#)]
55. Li, X.; Xia, M.; Dong, X.; Long, R.; Liu, Y.; Huang, Y.; Long, S.; Hu, C.; Li, X. High Mechanical Properties of Stretching Oriented Poly(butylene succinate) with Two-Step Chain Extension. *Polymers* **2022**, *14*, 1876. [[CrossRef](#)] [[PubMed](#)]
56. Witt, U.; Yamamoto, M. Method for the Continuous Production Of Biodegradable Polyesters. US Patent 9040639 B2 (to BASF SE), 26 May 2015.
57. Larrañaga, A.; Lizundia, E. A review on the thermomechanical properties and biodegradation behaviour of polyesters. *Eur. Polym. J.* **2019**, *121*, 109296. [[CrossRef](#)]

58. Lee, H.J.; Cho, W.Y.; Lee, H.C.; Seo, Y.H.; Baek, J.W.; Lee, P.C.; Lee, B.Y. Rapid Biodegradable Ionic Aggregates of Polyesters Constructed with Fertilizer Ingredients. *J. Am. Chem. Soc.* **2022**, *144*, 15911–15915. [[CrossRef](#)]
59. Abe, T.; Kamiya, T.; Otsuka, H.; Aoki, D. Plastics to fertilizer: Guiding principles for functional and fertilizable fully bio-based polycarbonates. *Polym. Chem.* **2023**, *14*, 2469–2477. [[CrossRef](#)]
60. Chen, Z.s.; Liu, T.; Dong, J.f.; Chen, G.; Li, Z.; Zhou, J.l.; Chen, Z. Sustainable Application for Agriculture Using Biochar-Based Slow-Release Fertilizers: A Review. *ACS Sustain. Chem. Eng.* **2023**, *11*, 1–12. [[CrossRef](#)]
61. Mo, S.; Guo, Y.; Liu, X.; Wang, Y. Efficient depolymerization of PET over Ti-doped SBA-15 with abundant Lewis acid sites via glycolysis. *Catal. Sci. Technol.* **2023**, *13*, 6561–6569. [[CrossRef](#)]
62. Casey, É.; Breen, R.; Gómez, J.S.; Kentgens, A.P.M.; Pareras, G.; Rimola, A.; Holmes, J.D.; Collins, G. Ligand-Aided Glycolysis of PET Using Functionalized Silica-Supported Fe₂O₃ Nanoparticles. *ACS Sustain. Chem. Eng.* **2023**, *11*, 15544–15555. [[CrossRef](#)]
63. Yang, Y.; Sharma, S.; Di Bernardo, C.; Rossi, E.; Lima, R.; Kamounah, F.S.; Poderyte, M.; Enemark-Rasmussen, K.; Ciancaleoni, G.; Lee, J.-W. Catalytic Fabric Recycling: Glycolysis of Blended PET with Carbon Dioxide and Ammonia. *ACS Sustain. Chem. Eng.* **2023**, *11*, 11294–11304. [[CrossRef](#)]
64. Lee, J.J.; Jeon, J.Y.; Park, J.H.; Jang, Y.; Hwang, E.Y.; Lee, B.Y. Preparation of high-molecular-weight poly(1,4-butylene carbonate-co-terephthalate) and its thermal properties. *RSC Adv.* **2013**, *3*, 25823–25829. [[CrossRef](#)]
65. ASTM D882-18; Standard Test Method for Tensile Properties of Thin Plastic Sheeting. ASTM International: West Conshohocken, PA, USA, 2018.
66. 17556:19; Plastics—Determination of the Ultimate Aerobic Biodegradability of Plastic Materials in Soil by Measuring the Oxygen Demand in a Respirometer or the Amount of Carbon Dioxide Evolved. ISO: Geneva, Switzerland, 2019.
67. Deng, L.-M.; Wang, Y.-Z.; Yang, K.-K.; Wang, X.-L.; Zhou, Q.; Ding, S.-D. A new biodegradable copolyester poly(butylene succinate-co-ethylene succinate-co-ethylene terephthalate). *Acta Mater.* **2004**, *52*, 5871–5878. [[CrossRef](#)]
68. Devroede, J.; Duchateau, R.; Koning, C.E.; Meuldijk, J. The synthesis of poly(butylene terephthalate) from terephthalic acid, part I: The influence of terephthalic acid on the tetrahydrofuran formation. *J. Appl. Polym. Sci.* **2009**, *114*, 2435–2444. [[CrossRef](#)]
69. Lee, H.J.; Baek, J.W.; Kim, T.J.; Park, H.S.; Moon, S.H.; Park, K.L.; Bae, S.M.; Park, J.; Lee, B.Y. Synthesis of Long-Chain Branched Polyolefins by Coordinative Chain Transfer Polymerization. *Macromolecules* **2019**, *52*, 9311–9320. [[CrossRef](#)]
70. Park, S.Y.; Chun, J.; Jeon, J.Y.; Lee, P.C.; Hwang, Y.; Song, B.G.; Ramos, R.; Ryu, C.Y.; Lee, B.Y. Branched poly(1,4-butylene carbonate-co-terephthalate)s: LDPE-like semicrystalline thermoplastics. *J. Polym. Sci. Part A Polym. Chem.* **2015**, *53*, 914–923. [[CrossRef](#)]
71. Kyeremateng, S. Correlating rheological behavior with molecular weight of different pharmaceutical NaCMC grades. *J. Anal. Pharm. Res.* **2022**, *11*, 39–43.

Disclaimer/Publisher’s Note: The statements, opinions and data contained in all publications are solely those of the individual author(s) and contributor(s) and not of MDPI and/or the editor(s). MDPI and/or the editor(s) disclaim responsibility for any injury to people or property resulting from any ideas, methods, instructions or products referred to in the content.